Theor Appl Climatol
DOI 10.1007/s00704-010-0331-6

ORIGINAL PAPER

Simulated changes in the atmospheric water balance over South Asia in the eight IPCC AR4 coupled climate models

Venkatraman Prasanna · Tetsuzo Yasunari

Received: 1 April 2009 / Accepted: 19 August 2010

Abstract This paper evaluates the performance of eight state-of-art IPCC-AR4 coupled atmosphere-ocean general circulation models in their representation of regional characteristics of atmospheric water balance over South Asia. The results presented here are the regional climate change scenarios of atmospheric water balance components, precipitation, moisture convergence and evaporation (*P*, *C* and *E*) up to the end of the twenty-second century based on IPCC AR4 modelling experiments conducted for (A1B) future greenhouse gas emission scenario. The AOGCMs, despite their relatively coarse resolution, have shown a reasonable skill in depicting the hydrological cycle over the South Asian region. However, considerable biases do exist with reference to the observed atmospheric water balance and also inter-model differences. The monsoon rainfall and atmospheric water balance changes under A1B scenario are discussed in detail. Spatial patterns of rainfall change projections indicate maximum increase over north-west India in most of the models, but changes in the atmospheric water balance are generally widespread over South Asia. While the scenarios presented in this study are indicative of the expected range of rainfall and water balance changes, it must be noted that the quantitative estimates still have large uncertainties associated with them.

V. Prasanna · T. Yasunari
Hydrospheric Atmospheric Research Center (HyARC),
Nagoya University,
Nagoya, Japan

Present Address:
V. Prasanna (✉)
International Pacific Research Center, SOEST,
University of Hawaii at Manoa,
Honolulu, Hawaii
e-mail: prasa_arnala@yahoo.com

1 Introduction

The Intergovernmental Panel on Climate Change (IPCC) scientific assessment reports (IPCC 1996, 2001, 2007; Christensen et al. 2007) present scientific evidence that human activities may already be influencing the climate. If one wishes to understand, detect and eventually predict the human influence on climate, one need to understand the system that determines the climate of the earth and of the processes that lead to climate change. The regional climatic impacts associated with global climatic change and their assessments are gaining increasing importance. This is because the agriculture, water resources, ecology etc., are vulnerable to climatic changes on regional scale.

Climate variations and change, caused by external forcings, may be partly predictable, particularly on the larger (e.g. continental, global) spatial scales. Because human activities, such as the emission of greenhouse gases or land-use change, do result in external forcing, it is believed that the large-scale aspects of human-induced climate change are also partly predictable. However, the ability to actually do so is limited because we cannot accurately predict population change, economic change, technological development, and other relevant characteristics of future human activity. In practice, therefore, one has to rely on carefully constructed scenarios of human behaviour and determine climate projections on the basis of such scenarios.

Several model intercomparison efforts have been made to resolve the major issues in realistically simulating the Asian summer monsoon precipitation. The most prominent and relevant include the Atmospheric Model Intercomparison Project (Gates et al. 1999; Gadgil and Sajani 1998; Kang et al. 2002; Waliser et al. 2003; Wang et al. 2004) and the Coupled Model Intercomparison Project (Lambert and Boer 2001; Covey et al. 2003). These studies bring out the

Published online: 06 September 2010

strengths and shortcomings of both atmospheric and coupled models as regarding their ability in simulating both the circulation and the precipitation on global and regional scales. However, this paper brings out the strength of coupled atmosphere-ocean general circulation models (AOGCMs) in simulating the regional hydrological cycle over South Asia and uncertainties involved in these simulations.

The results of several AOGCM simulations are presented for the South Asian monsoon region, to provide an idea of their skill in representing the regional hydrological cycle and their future projections. Datasets used in the study are from IPCC-AR4 simulations of AOGCMs forced with reconstructed greenhouse gas and aerosol concentrations to represent the present day climate (20C3m) and future concentrations according to the Special Report on Emission Scenario (SRES) A1B. The likely future changes in rainfall and associated hydrological cycle over the South Asian region are presented. In order to provide the essential background, a brief description of the observed hydrological cycle over the South Asian region is presented using observed and reanalysis datasets before discussing the future scenarios of atmospheric water balance (AWB) over South Asia.

The water balance method provides an opportunity to effectively study the hydrological cycle at each grid point on the regional scale through the balance. The simulated water balance components are compared with the observed precipitation and the moisture convergence computed from the reanalysis dataset. Here attempt has been made to utilize the best available precipitation (P) and convergence (C) computed from the reanalysis dataset. Considering the South Asian monsoon region in the domain of 0–30N and 65–100E in each reanalysis and AOGCM, the area averages of precipitation, convergence and evaporation fields are worked out to generate monthly data for the considered periods of the AOGCM simulations. These monthly data are then used to compute the seasonal totals of P, C and evaporation (E). Taking 1980–1999 as the baseline period, the seasonal quantities are then examined for their likely future changes into the twenty-first and twenty-second centuries.

Following the seminal works on global water budget studies (Trenberth 1991; Oki et al. 1995; Trenberth and Guillemot 1998; Trenberth 1999); Prasanna and Yasunari (2008, 2009) studied the water balance over South Asian monsoon region and found that the role of evaporation is also crucial for understanding the interannual variability of precipitation over this region. They have pointed out that the contribution of evaporation to precipitation is as large as that of convergence over both dry and wet regimes. So the contribution of evaporation cannot be simply neglected when we consider projections based on AOGCM results.

The structure of this paper is as follows. Section 2 describes the datasets and methodology. Section 3 discusses the observed water balance over South Asia. Section 4 presents a discussion of the simulated hydrological cycle over South Asia by AOGCMs. In Section 5, we document the climate change simulations of water balance over South Asia in eight AOGCMs. Section 6 presents the discussion and main conclusions.

2 Datasets and methodology

The transient climate change simulations of eight AOGCMs have been used in the present study. These climate change simulations are part of the suite of simulations performed for the IPCC AR4 scientific assessment report, and the data have been obtained from the Program for Climate Model Diagnosis and Intercomparison (PCMDI) at the Lawrence Livermore National Laboratory (LLNL), USA. The main centres of development of the eight models used in the study, along with their acronyms are listed in Table 1. The technical details of the above AOGCMs, including resolution and various physical parameterization schemes are summarized in the references quoted in Table 1. The eight models have been used to simulate global climate representing the present climate (20C3M) and the likely future changes with A1B forcing.

2.1 Model experiments

Scenarios are among the main methods used to address the complexity and uncertainty of future challenges associated with climate change. The IPCC initiated the development of greenhouse gas emission scenarios designed to serve as inputs to GCMs and facilitate the assessments of climate change impacts (IPCC 1996). The simulation experiments used in the present study indicated below are

(1) 20C3M Run
The 20C3M run is a control integration, in which the atmospheric forcing in terms of the greenhouse gas concentration is taken from reconstructed time series of concentrations and performed for a period of roughly 150 years, typically 1860–2000. The climatology constructed is from the last 20 years of the 20C3M run to represent the present day climate (1980–1999) in each model.

(2) A1B Scenario
A1B scenario falls in the category of 'Medium-High emission scenario'. The scenario family describes a future world of very rapid economic growth, global population that peaks in mid-century and declines thereafter, and the rapid introduction of new and more efficient technologies, with a substantial reduction in regional differences in per capita income and a balanced usage of fossil and non-fossil fuels (IPCC 2001).

Table 1 Description of eight-coupled climate model simulations used in the study

Model name	IPCC, ID	Centre	Reference
CCMA	CGCM3.1 (t47)	Canadian Centre for Climate Modelling and Analysis, Canada	Flato et al. (2000)
CNRM	CNRM-CM3	Meteo-France/Centre National de Recherches, France	Salas-Melia et al. (2005)
GFDL	GFDL-CM2.0	Geophysical Fluid Dynamics Laboratory, USA	Delworth et al. (2006)
MPI	ECHAM5/MPI-OM	Max Planck Institute for Meteorology, Germany	Jungclaus et al. (2006)
MRI	MRI-CGCM2.3.2	Meteorological Research Institute, Japan	Yukimoto et al. (2001)
HADCM	UKMO-HadCM3	Hadley Centre for Climate, UK	Jones et al. (2004)
HADGEM	UKMO-HadGEM1	Hadley Centre for Climate, UK	Johns et al. (2006); Jones et al. (2004)
INMCM	INM-CM3.0	Institute for Numerical Mathematics, Russia	Diansky and Volodin (2002)

Monthly data of P and E from AOGCMs (Table 1) are utilized for 20C3M run and A1B scenario. The lengths of the data for each model run are 240 months for 20C3M simulation to correspond with the present climate of 1980–1999 (i.e. last 20 years of 20C3M run of each model) and 2,400 months simulation of A1B (i.e. 200 years representing 2000–2200). The data have been downloaded from the PCMDI—LLNL (http://www-pcmdi.llnl.gov/). Due to data limitations, results are presented only for eight models for 20C3M and A1B scenarios. The moisture C for each model is obtained from P and E, as the model is balanced throughout the runs.

Six hourly data from the National Center for Environmental Prediction-National Center for Atmospheric Research (NCEP/NCAR) reanalysis dataset (Kalnay et al. 1996) are used to calculate water budgets for the 20-year period starting from January 1980 up to December 1999. These data comprise of upper level winds (u, v), specific humidity (q), geopotential height (z), surface winds (u, v), surface level specific humidity (q) and sea level pressure (slp). In addition, GPCP precipitation estimate for both land and ocean is utilized in this study, as the precipitation estimates over land areas are quite realistic in GPCP (Adler et al. 2003) due to the merging of IR and microwave sensor estimates with the gauge precipitation estimates. Similar calculations are also done for the 40 years European centre for medium range weather forecasting (ECMWF) reanalysis (ERA-40) dataset (Uppala et al. 2005) and 25 years Japanese reanalysis (JRA-25) dataset (Onogi et al. 2000). But for the sake of brevity we used C computed from NCEP/NCAR reanalysis only for comparison with models in this study.

3 Observed water balance over South Asia

The most important feature in the global large-scale meteorology is the hydrological cycle over the tropics, especially the hydrological cycle over the Asian monsoon region. A simple schematic diagram of water balance over a small area on a longer time scale is shown in Fig. 1.

3.1 Water balance components

The atmospheric water budget equation can be written as (Peixoto and Oort 1992),

$$< \partial W/\partial t > + < \nabla \quad .Q >=< E-P > \tag{1}$$

Where $\boldsymbol{P}$ is precipitation, $\boldsymbol{E}$ is evaporation, $\boldsymbol{W}$ is precipitable water content, $\boldsymbol{Q}$ is vertically integrated moisture flux vector, $\nabla\cdot\boldsymbol{Q}$ its divergence and angled brackets denote the area average.

On longer timescales like monthly or seasonal, under near equilibrium conditions, the time change of local available precipitable water content is negligible compared with the variations of large-scale convergence and evaporation (Oki et al. 1995; Trenberth 1999).

$$< \partial W/\partial \mathrm{t} > \approx 0 \tag{2}$$

We can approximate,

$$P = C + E \tag{3}$$

Where,

$$C = - <\nabla\cdot Q>$$

Vertically integrated moisture flux vector is given by,

$$Q = 1/g_{\mathrm{Pt}} \int^{\mathrm{Ps}} \mathrm{qvdp} \tag{4}$$

C is computed by performing vertical integration from ground (surface pressure level) to 300 hPa for all the standard atmospheric pressure levels.

The C in the observation case is obtained from the vertical integration, where as the C in the model is obtained

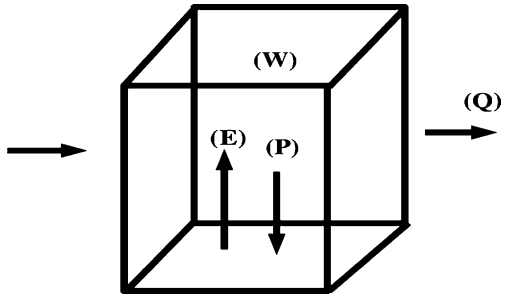

Fig. 1 A simple Schematic diagram showing water balance over a small area on a longer time scale, where P is the precipitation, Q is the vertically integrated moisture flux. E is the evaporation from surface; W is the precipitable water content. $C = -\langle \nabla \cdot Q \rangle$

from the atmospheric water balance equation [$C=P-E$] as the components are balanced in the coupled model runs. The sign of convergence and divergence are reversed in this study for convenience. The E in the observation case is obtained as a residual between observed P and the C computed from the respective reanalyses, since the P from GPCP is reliable than the P obtained from the reanalyses.

In principle C has to be calculated on the model time step, so that using 6-hourly values from the reanalyses leads to some unknown uncertainty in the absolute values of C. But we believe that the calculated convergence from 6-hourly data is acceptable to conduct a comparison with coarse resolution AOGCM results, especially as the large-scale patterns of C are rather similar in the three reanalyses (see Fig. 2).

3.2 Computed large-scale convergence from reanalyses

The moisture convergence computed from the three major reanalyses are shown in Fig. 2 for comparison. The large-scale convergences computed from different reanalysis dataset differ considerably due to the differences in the data assimilated over a specific region and also over data sparse regions. The data over data sparse region is filled with the first guess of the model, so that such regions like oceans are completely model dependent. The regions with dense observations will have high reliability, for example over continental regions where observations of upper levels are adequate compared with areas over oceans. Results from this study and from the expert references yielded that ERA-40 has problems over the regions close to tropics. The ERA-40 has estimated strong convergence over oceans and strong divergence over land (Hagemann et al. 2005). Some problems and deficiencies of the column integrated water vapour in NCEP/NCAR are also highlighted by Trenberth et al. 2005. However the gross features of moisture convergence and monthly annual cycle are captured well over the South Asian region in all three major reanalyses. To reassure our confidence, we compared calculated moisture C from all three reanalysis datasets.

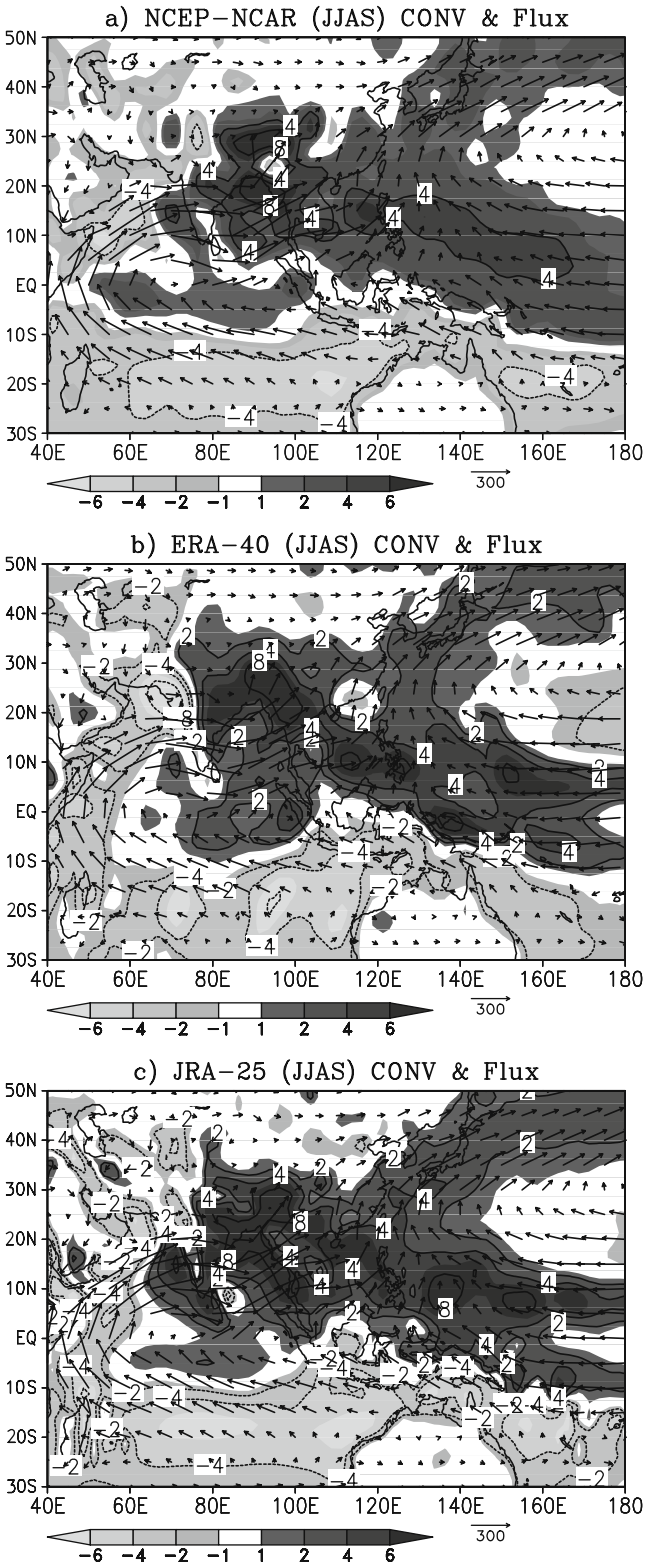

Fig. 2 Moisture convergence (mm/day) and moisture flux vectors ($kg^{-1}m^{-1}s^{-1}$) computed for JJAS season from three major reanalyses for the period 1980–1999

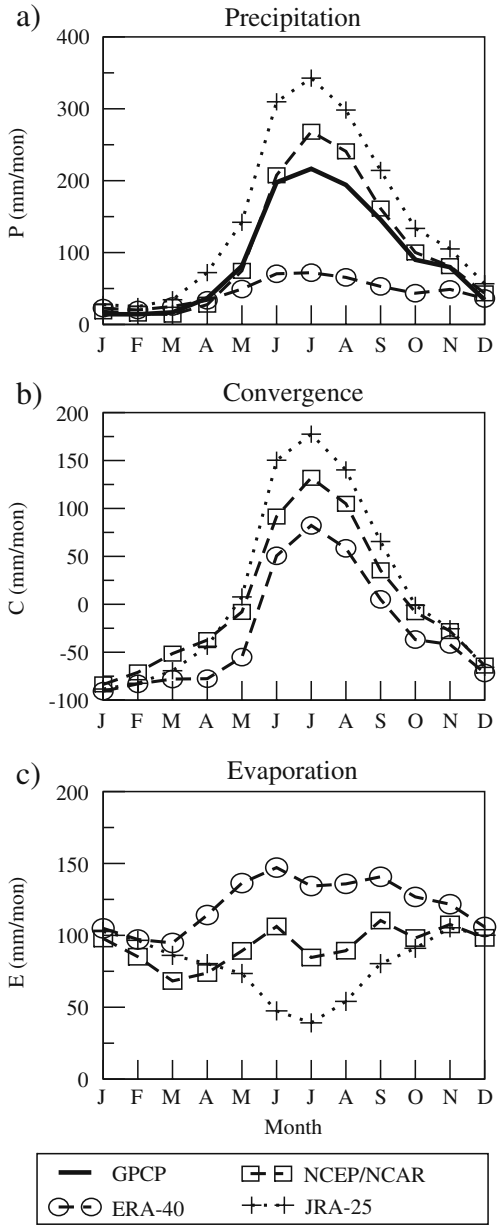

Fig. 3 Observed annual cycle of atmospheric water balance (P, C and E) (mm/month) over South Asia

3.3 Contribution of *C* and *E* to *P*

Major portion of precipitation over the South Asian monsoon region is realized within the 4 months JJAS (Fig. 3a), divergence prevails until early May and net divergence becomes net convergence over the large domain of South Asia from the month of May (Fig. 3b). The monsoon rains are contributed equally by *C* and *E* during monsoon months JJAS in the NCEP/NCAR reanalysis, where as $E>C$ in ERA-40 reanalysis and $C>E$ in JRA-25 reanalysis (Fig. 3b, c). These results show that convergence is very strong in JRA-25 and divergence is very strong in ERA-40 and NCEP/NCAR is in between JRA-25 and ERA-40 reanalyses.

4 Simulation of hydrological cycle over South Asia by AOGCMs

4.1 Observed and simulated precipitation and convergence climatology

The large-scale South Asian monsoon precipitation and convergence patterns in the summer (JJAS), as simulated by the eight-coupled models, are shown in Figs. 4 and 5, respectively. For this purpose, the long-term means of seasonal precipitation and convergence have been computed based on all available observation datasets and 1980–1999 (20C3M) control simulations. The simulated rainfall patterns are compared with the observed precipitation of GPCP (Global Precipitation Climatology Project) (Adler et al. 2003) for the period 1980–1999. While most models simulate the general maximum precipitation over west coasts of India and Bay of Bengal, some of them miss the rainfall maximum in the equatorial Indian Ocean. Apart from this, in the Indian monsoon context, the observed maximum rainfall during the monsoon season along the west coast of India and the North Bay of Bengal and adjoining northeast India is not quite realistically simulated in many models except GFDL and to some extent in CCMA, MPI, HADCM and MRI (Fig. 4). This may possibly be linked to the coarse resolution of the models as the heavy rainfall over these regions is generally in association with the steep orography. Similarly the moisture convergence pattern is not realistically simulated in many models except GFDL and to some extent in CCMA, MPI, HADCM and MRI (Fig. 5).

Most of the models miss the equatorial Indian Ocean precipitation maximum, except (GFDL) and to some extent in MRI, CNRM and INMCM (Fig. 4), which is also evident from the moisture convergence pattern (Fig. 5). Only GFDL model could reproduce the observed precipitation pattern and moisture convergence quite well over South Asia. Moreover, large inter-model differences are noted among the models.

4.2 Annual cycles of observed and simulated precipitation and convergence

Observed (GPCP) and simulated annual cycles of precipitation are shown in Fig. 6 where the precipitation is averaged over the South Asian region (land and sea) comprising 0N–30N and 65E–100E. The simulated precipitation shows remarkably similar patterns to the observed. Over the course, the precipitation changes from less than

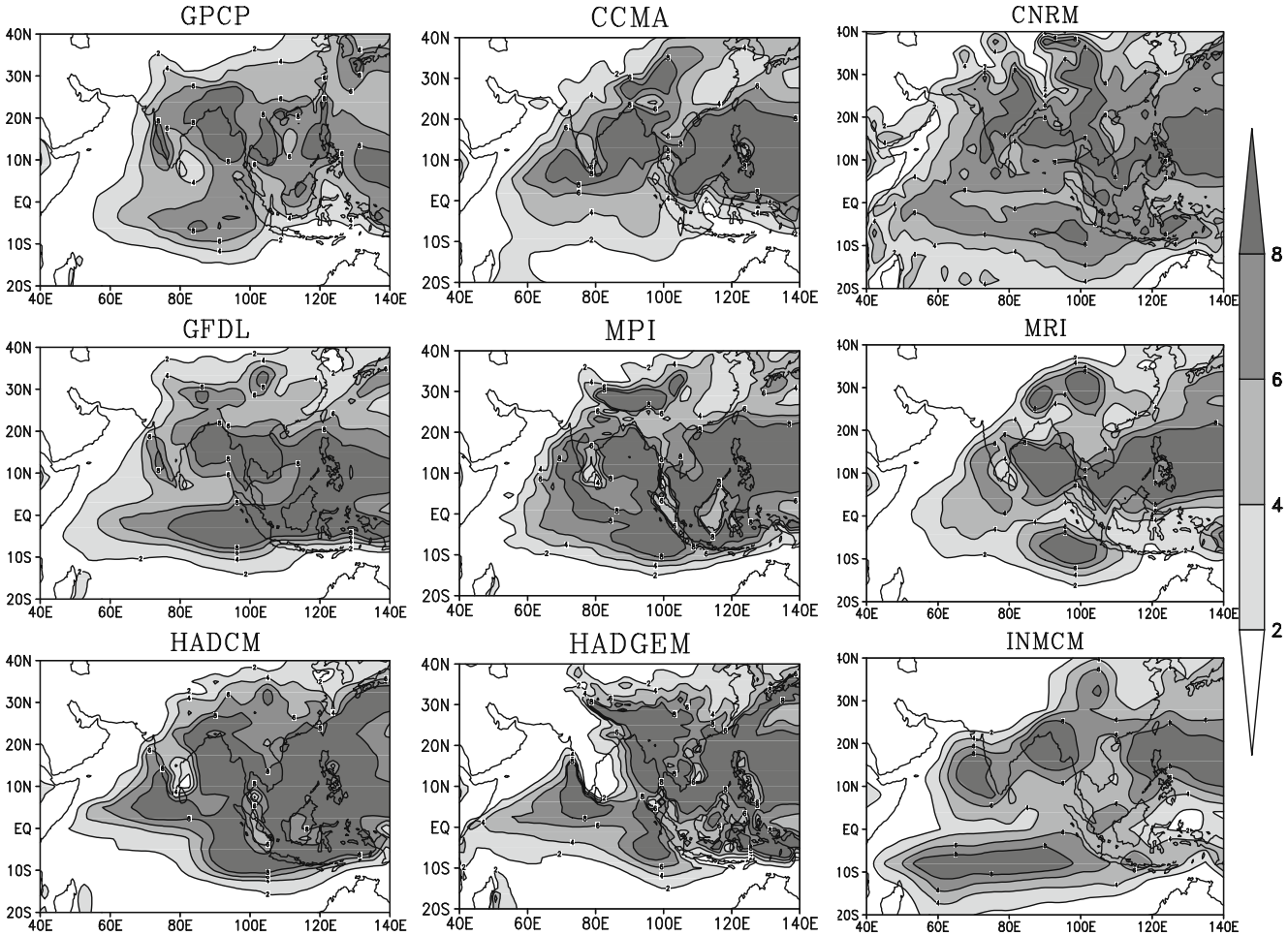

Fig. 4 Simulations of JJAS mean rainfall (mm/day) in the eight IPCC-AR4 models

50 mm/month during the January–April period to more than 200 mm/month during the peak summer monsoon period of June–August. Thus the annual cycle is characterized by a sharp increase from April to June and thereafter a gradual decrease from September. An examination of the model simulations (Fig. 6) suggests that

1. Three models (CCMA, CNRM and MPI) simulate a similar annual cycle in terms of shape and magnitude to observed characteristics. However, CNRM simulates excess precipitation during November and December.
2. Two models (HADGEM and MRI) simulate the shape of the annual cycle well but underestimate precipitation amounts, in particular during the spring and the summer periods.
3. Three models (GFDL, HADCM and INMCM) simulate peak rainfall a month later than observed, resulting in the underestimation of rainfall during spring and summer.

The estimated and simulated annual cycles of convergence for the eight models are shown in Fig. 7. The observed and simulated patterns of convergence resemble the observed and simulated patterns of precipitation.

1. Three models (CCMA, CNRM and MPI) simulate a similar annual cycle of convergence in terms of shape and magnitude to observed characteristics; also CNRM simulates excess convergence during November–December.
2. Two models (HADGEM and MRI) simulate the shape of the annual cycle well but underestimate convergence.
3. Three models (GFDL, HADCM and INMCM) simulate peak convergence a month later than observed.

The peak values of convergence (Fig. 7) in the model simulation and observation are roughly around 150 mm/month, where as the peak values of precipitation during summer season are roughly around 250 mm/month. The balance of roughly about 100 mm/month may come from the evaporation through in situ surface hydrological processes.

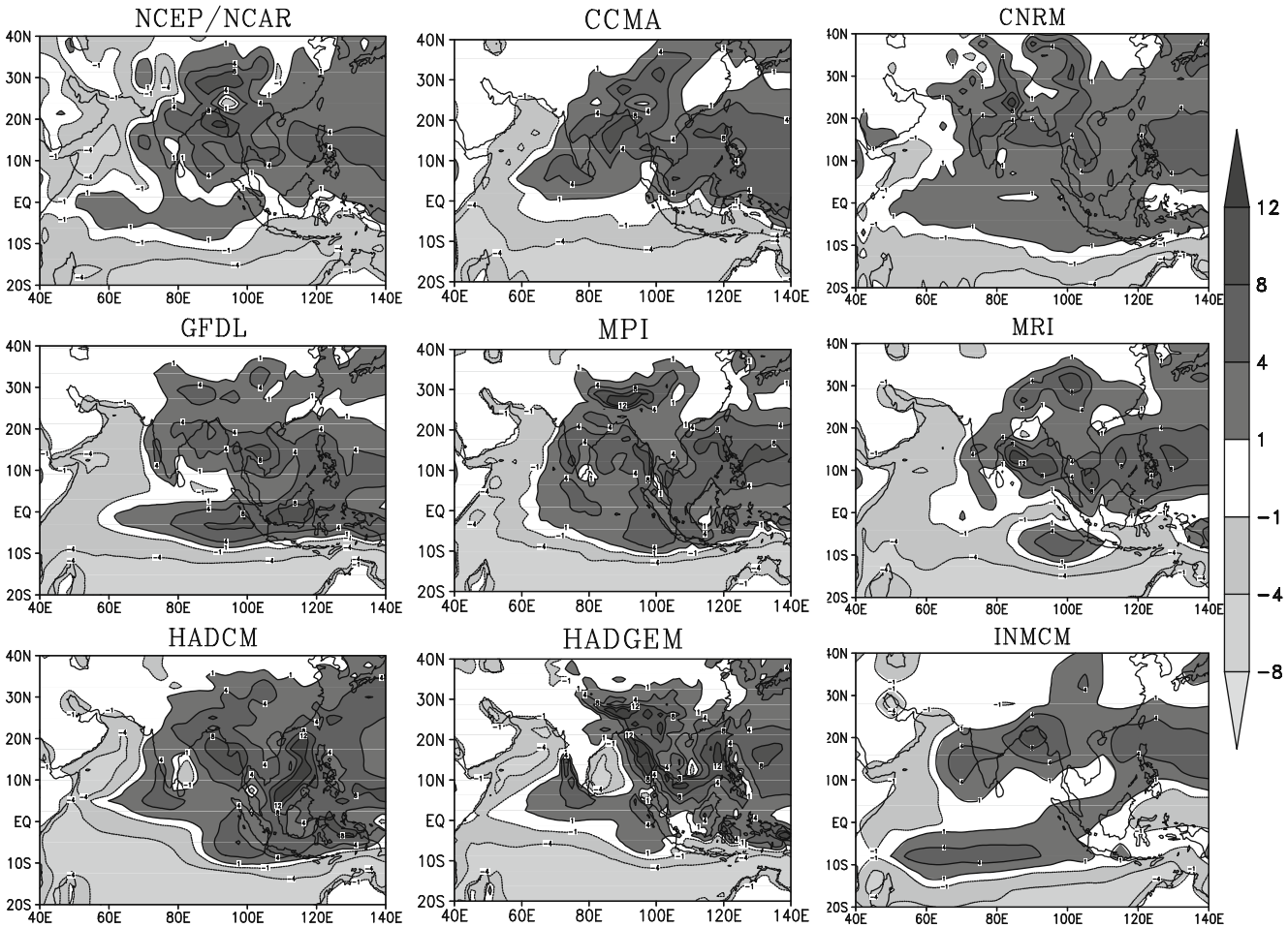

Fig. 5 Simulations of JJAS mean moisture convergence (mm/day) in the eight IPCC-AR4 models

5 Climate change simulations of water balance over South Asia in eight AOGCMs

The current generation of climate models reproduces the major features of the observed distribution of the *P* and *C* to some extent, but there is nevertheless, a considerable scatter among model results and between simulated and observed values. The time series of simulated South Asian summer monsoon rainfall are shown in Fig. 8 for 20C3m and the A1B scenario. The thick lines represent values smoothed with a 9-year moving average for each model respectively. As might be expected, in the 20C3M experiments with observed greenhouse forcing, the simulations of all models show very little resemblance to the observations of GPCP in the twentieth century. On the other hand, the transient simulations with A1B scenarios show marked increase in monsoon precipitation in the twenty-first and twenty-second centuries, particularly becoming obvious after the 2050s. As can be seen from Fig. 8, though all models show increase in precipitation over South Asia—there is a considerable spread among the models in the magnitude of change.

Comparison of AWB between observed and model simulations in the 20C3M and the subsequent changes in the future (A1B-20C3M) for JJAS over South Asian monsoon domain are shown in Fig. 9. All models show a general consensus of increase in the precipitation. The increase in mean precipitation is mainly due to the increase in the projected moisture convergence (Fig. 9) attributed to the horizontal transport of moisture from the oceans towards land through advection, which is consistent with earlier studies by Ueda et al. 2006 and Kripalani et al. 2007. The role of evaporation through insitu surface hydrological processes cannot be ruled out completely. The projected increase in the mean precipitation is evident in all the AOGCM results, while increases are large for moisture convergence but not for evaporation (Fig. 9).

5.1 Spatial patterns of changes in the atmospheric water balance over South Asia

The future rainfall changes on a broad regional scale described above are examined further to see their spatial

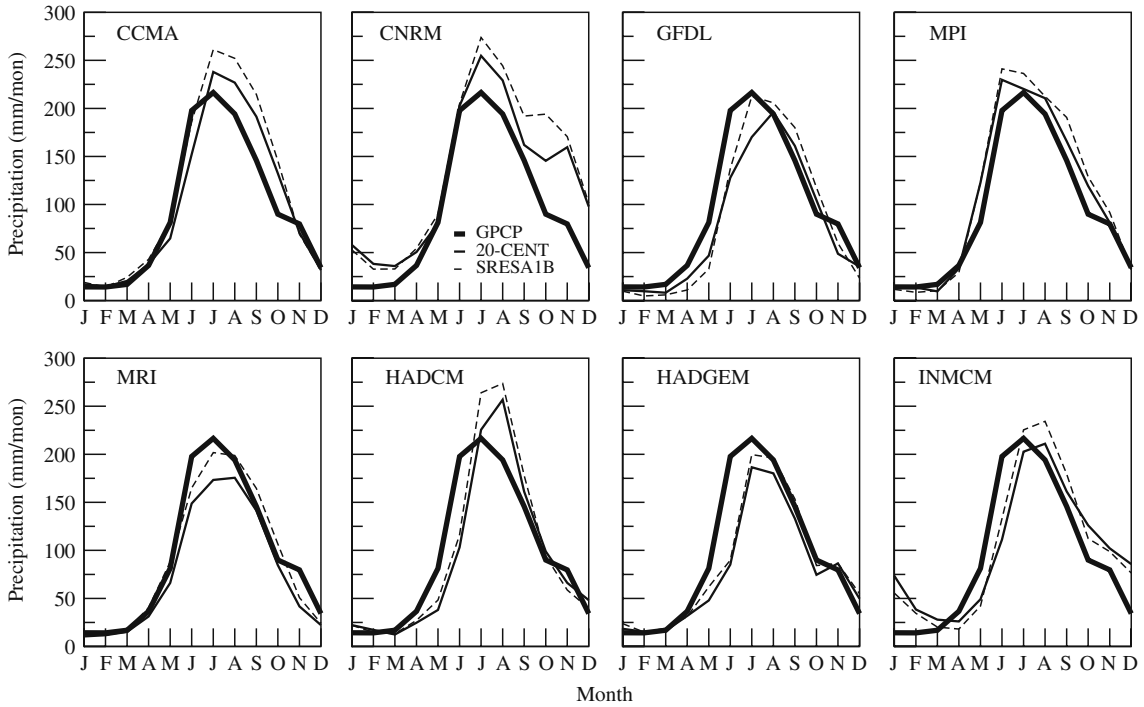

Fig. 6 Annual cycles of observed and simulated rainfall (mm/month) over South Asia in the 20C3M and A1B runs

manifestation over the South Asian region. The A1B forced changes in monsoon rainfall are computed for 200-years period starting 2000 to 2200 for all models and for 20-year period starting 1980 to 2000 in the 20C3M. The changes are expressed as percentage departure for the water budget components *P*, *C* and *E* (Figs. 10, 11 and 12) with reference to the present period (1980–1999) of 20C3M AOGCM simulations, considered as the baseline climate. As can be seen from Fig. 10, most of the models project an enhanced precipitation during the monsoon season, particularly over

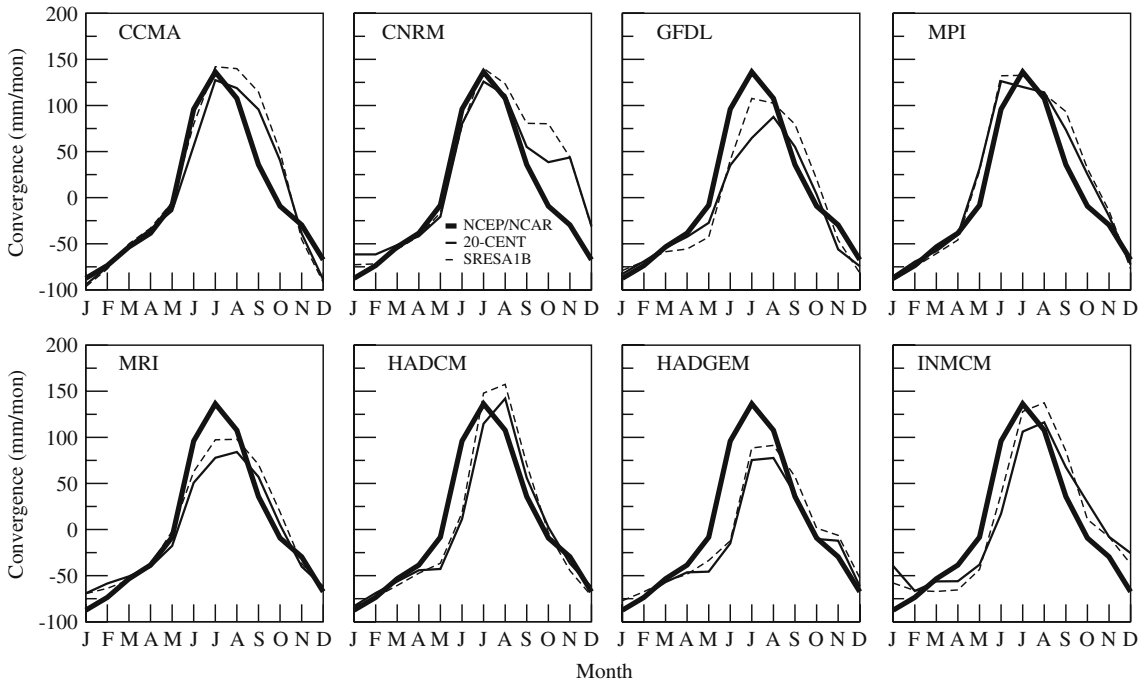

Fig. 7 Annual cycles of observed and simulated moisture convergence (mm/month) over South Asia in the 20C3M and A1B runs

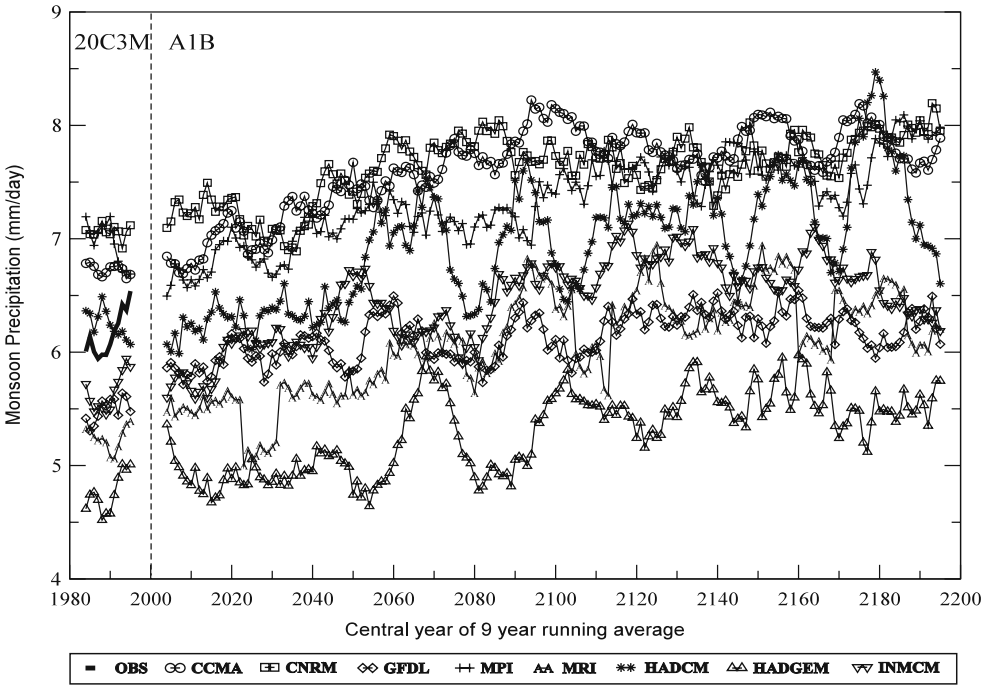

Fig. 8 Variation of South Asian monsoon rainfall (mm/day) simulated in the eight IPCC-AR4 models from 1980 to 2200

the northwestern parts of India. However, the magnitudes of projected change differ considerably from one model to the other. There is very little or no change noted in the monsoon rainfall over a major part of India. It is important to note here that the maximum change in rainfall is occurring over the climatologically low rainfall region of northwest India. The implications of such change over this region have to be carefully assessed in future studies.

GFDL and MPI model simulations show general decrease in precipitation over North West India, which is evident from the precipitation change (Fig. 10) due the decrease in both *C* and *E* (Figs. 11 and 12). Whereas, the HADCM and HADGEM model simulations show decrease in precipitation over South peninsular India (Fig. 10) due to decrease in *C* and *E* (Figs. 11 and 12). Generally increases in the precipitation over the South Asian region are accompanied

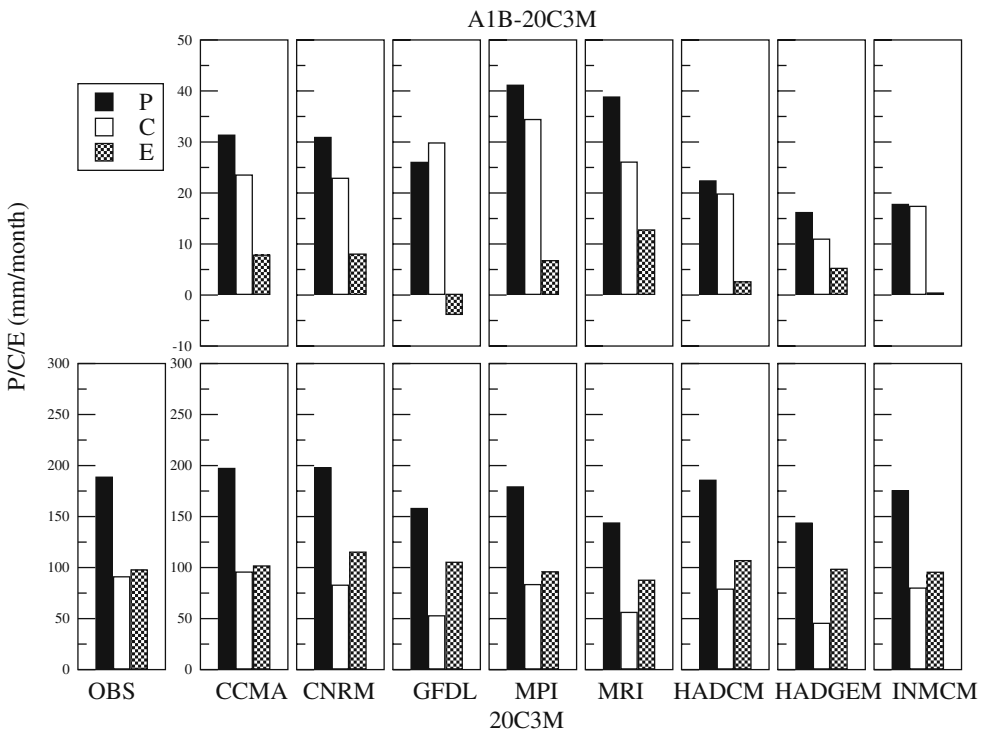

Fig. 9 Seasonal mean (JJAS) of AWB components (P, C and E) (mm/month) for different models in 20C3M and A1B Scenario runs. Bottom Panel shows observation and 20C3M run (1980–1999). Top panel shows difference between A1B runs and 20C3M runs. For observational AWB P is from GPCP, C is from NCEP/NCAR and E is a residual from P and C

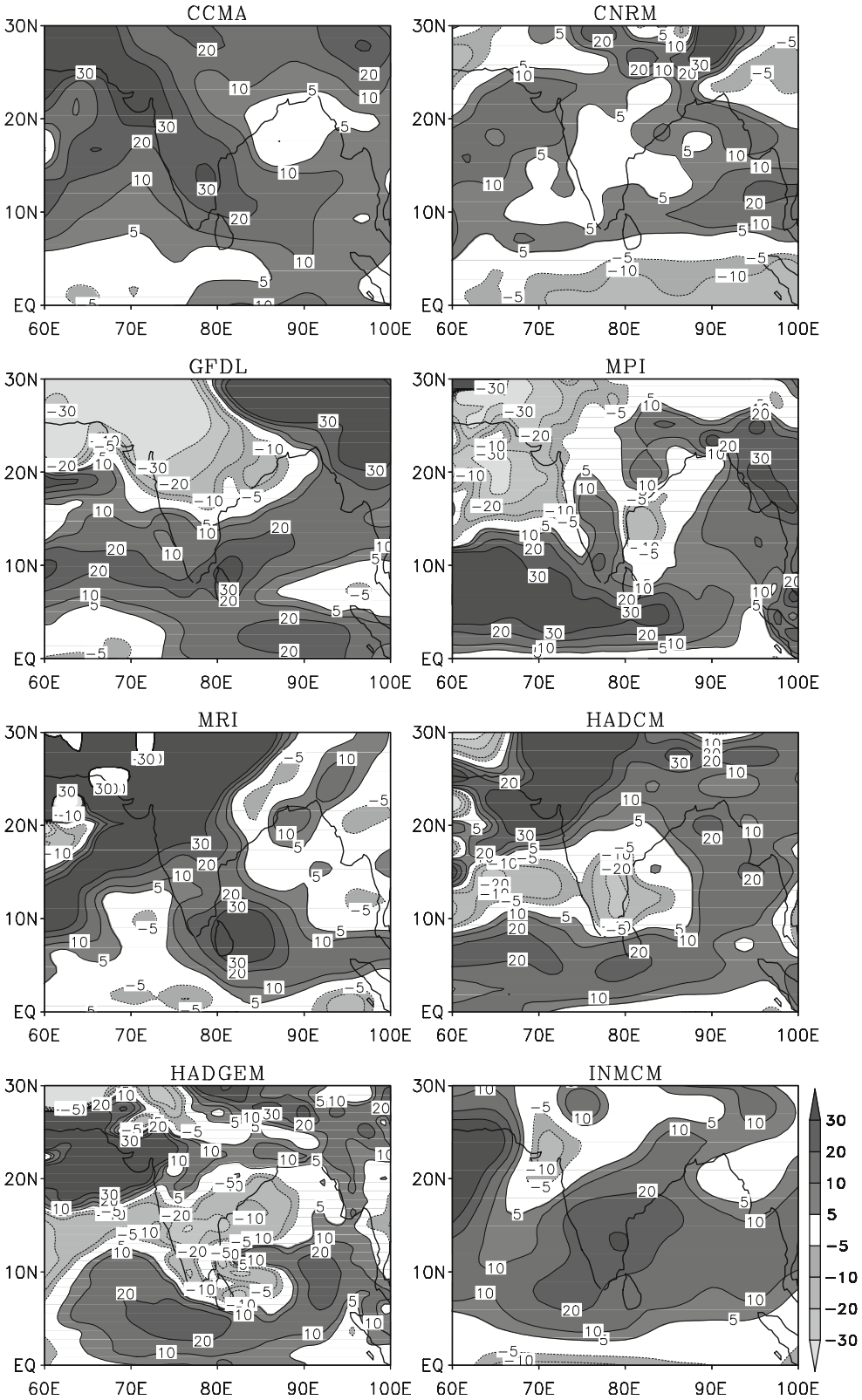

Fig. 10 Spatial patterns of projected monsoon rainfall changes (A1B–20C3M) in percentage departure

by increases in convergence as well as evaporation over the land area.

The changes in the moisture flux convergence are examined in detail using 850 hPa level winds and 850 hPa level tropospheric humidity. The 850 hPa wind changes for A1B scenario are shown in percentage departures from 20C3M (Fig. 13). Most of the models show decreases in the cross-equatorial flow and subsequent

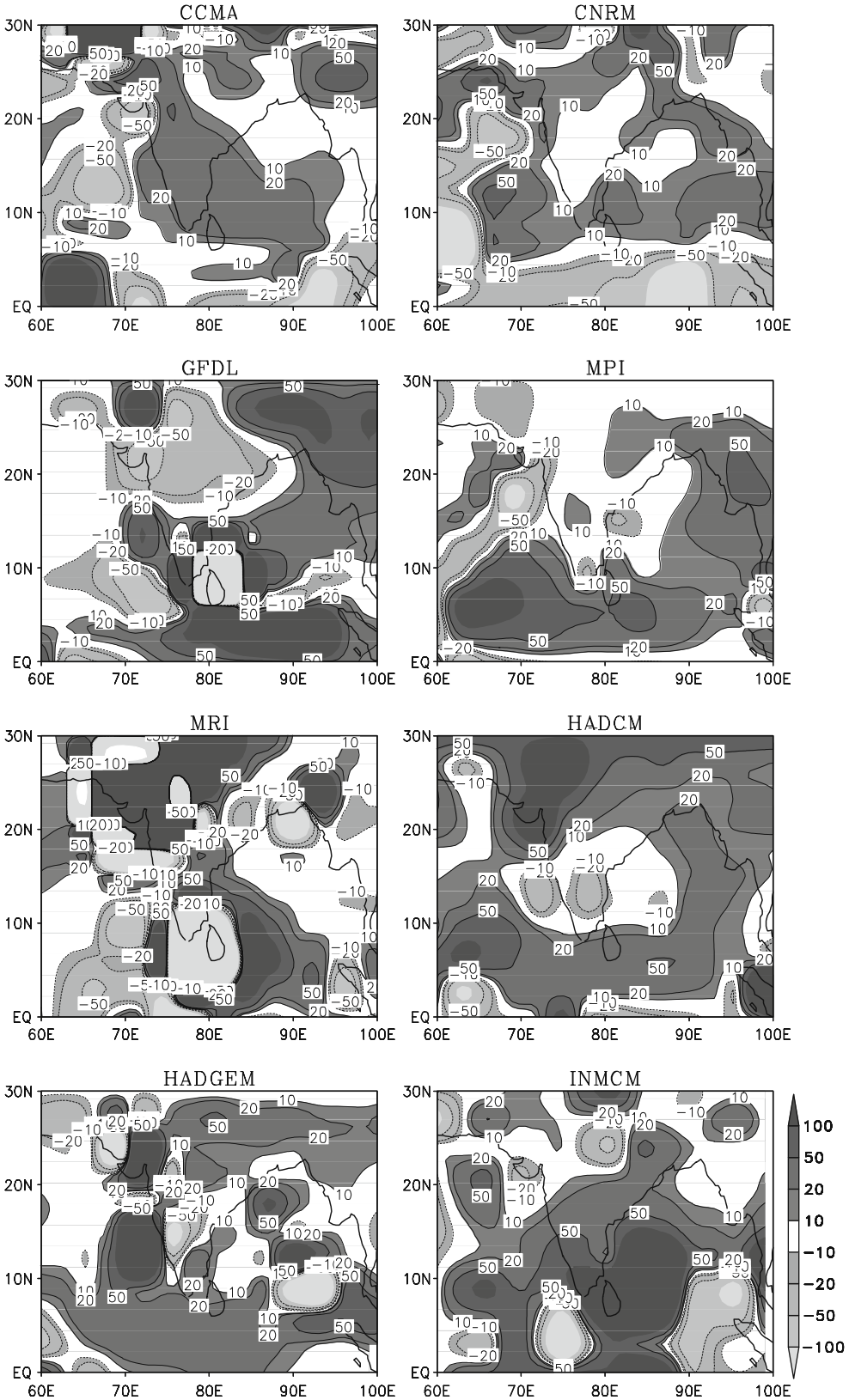

Fig. 11 Spatial patterns of projected convergence changes (A1B–20C3M) in percentage departure

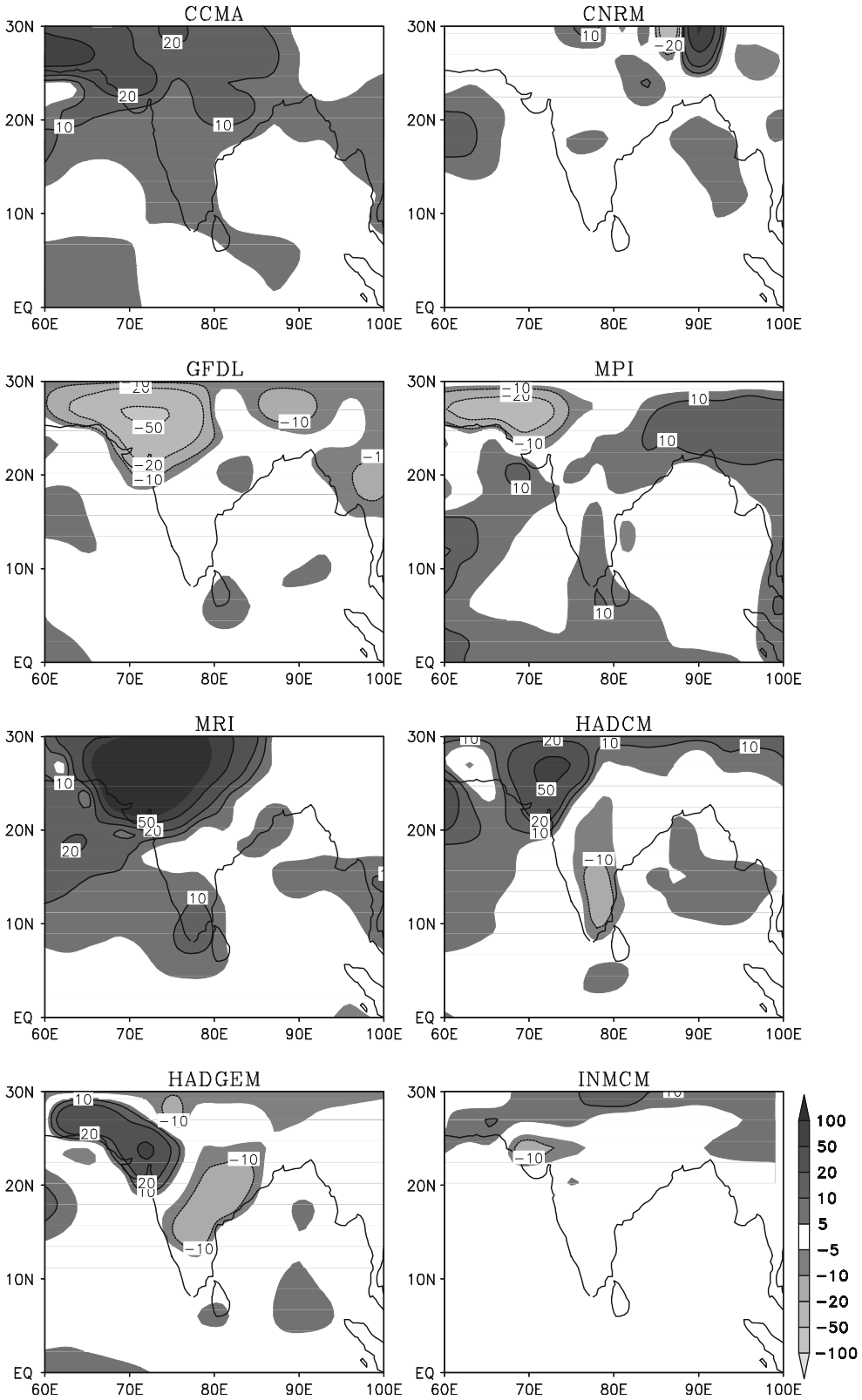

Fig. 12 Spatial patterns of projected evaporation changes (A1B–20C3M) in percentage departure

decrease in the winds over South Asia, which leads to decrease in the wind convergence over the South Asian monsoon region. Also, the specific humidity changes for A1B scenario are shown in percentage departures from 20C3M (Fig. 14). The specific humidity increase over South Asia is consistent in all models. We have also shown the 850-hPa moisture flux change for A1B scenario in total seven models (for HADCM model the specific humidity

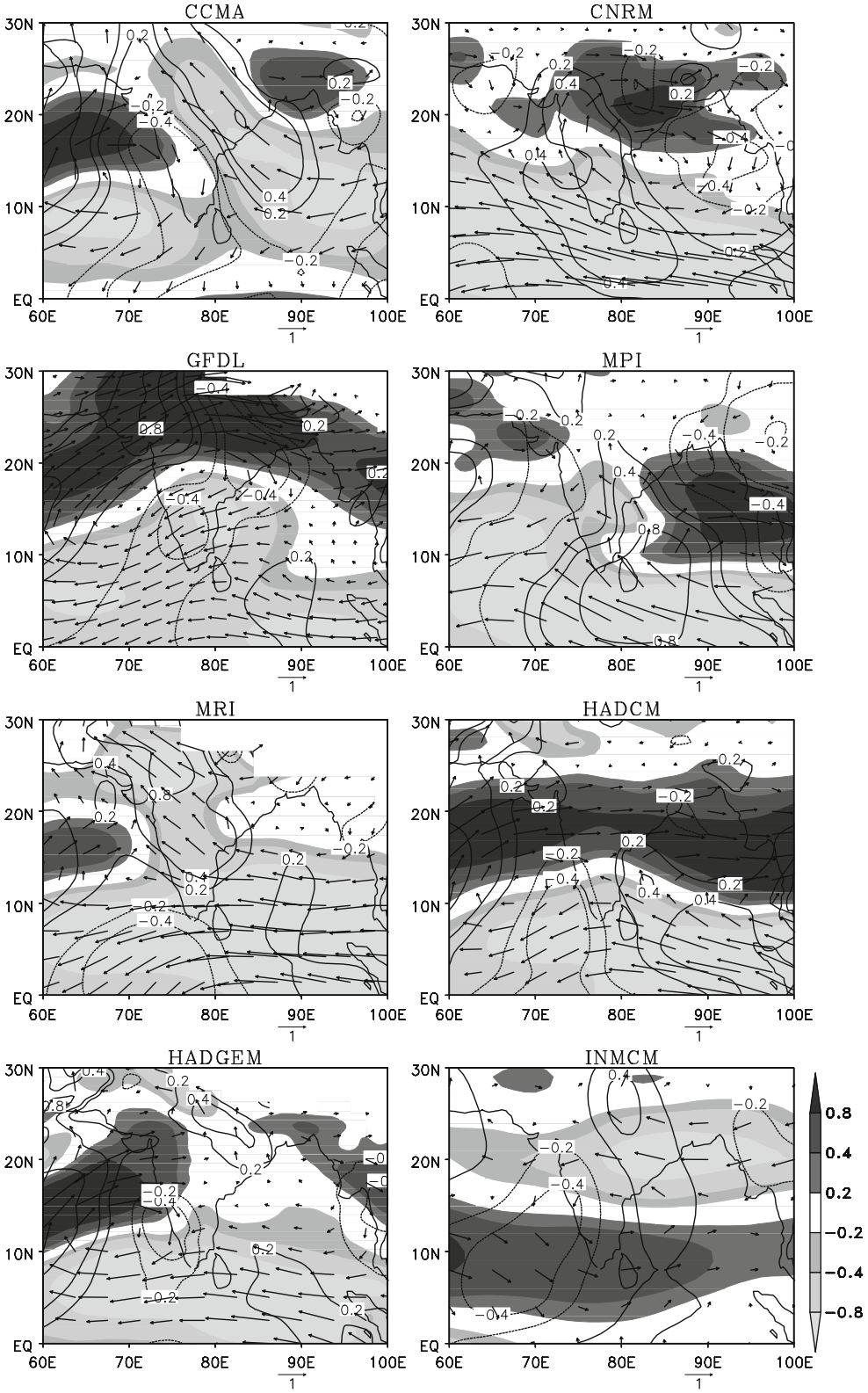

Fig. 13 Spatial patterns of projected 850 hPa wind changes (A1B–20C3M) in (m/s). Shaded values are differences in zonal wind and contour values are differences in meridional wind

fields were not available) in percentage departures from 20C3M (Fig. 15). The increase in moisture convergence flux can be attributed to the increase in the lower tropospheric specific humidity, which is evident in all models. Therefore P increase in the models is due to the increase of C due to increase in the lower tropospheric precipitable water component (PW) and not the wind convergence.

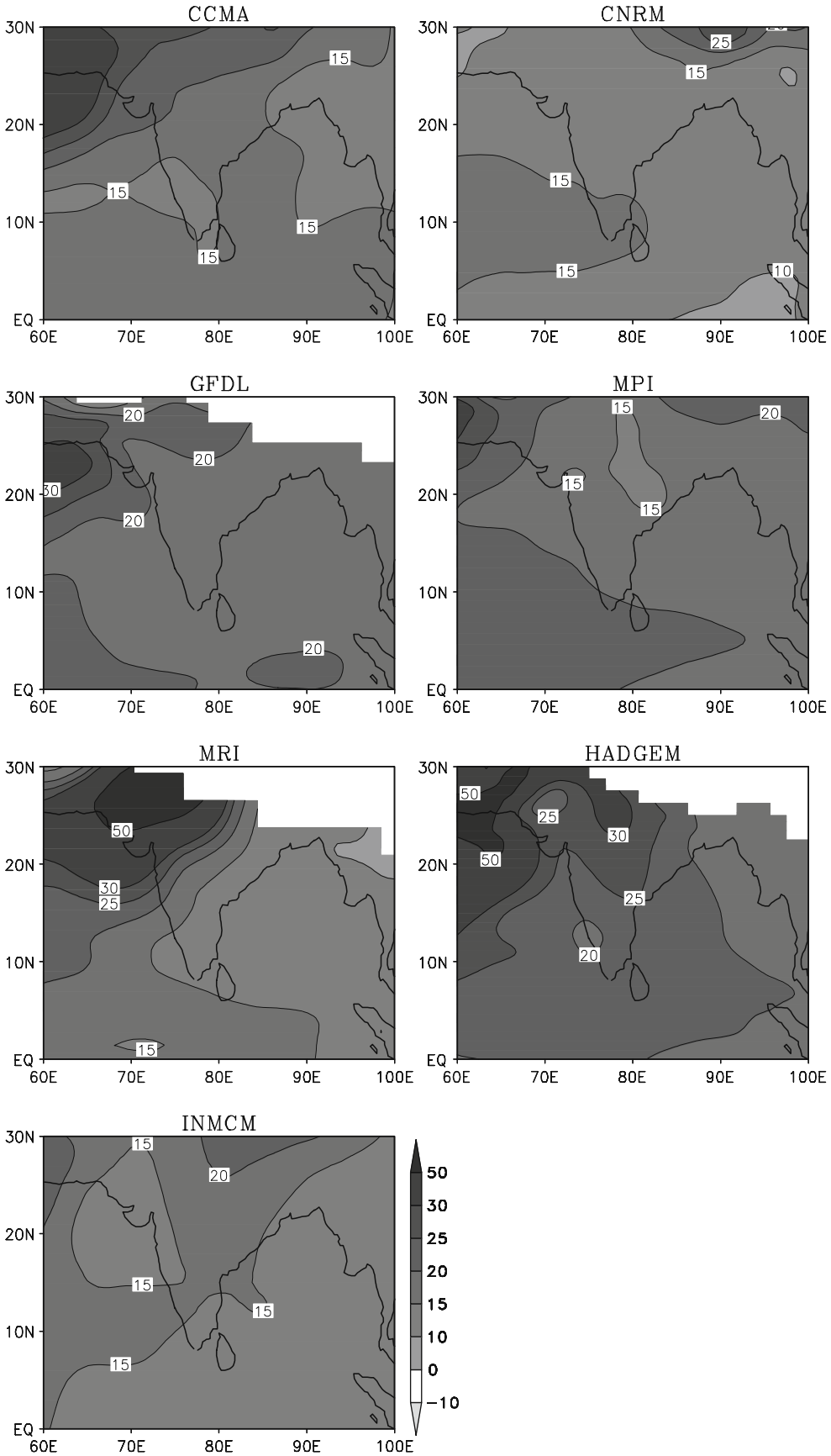

Fig. 14 Spatial patterns of projected 850 hPa specific humidity changes (A1B–20C3M) in percentage departure (kg/kg)

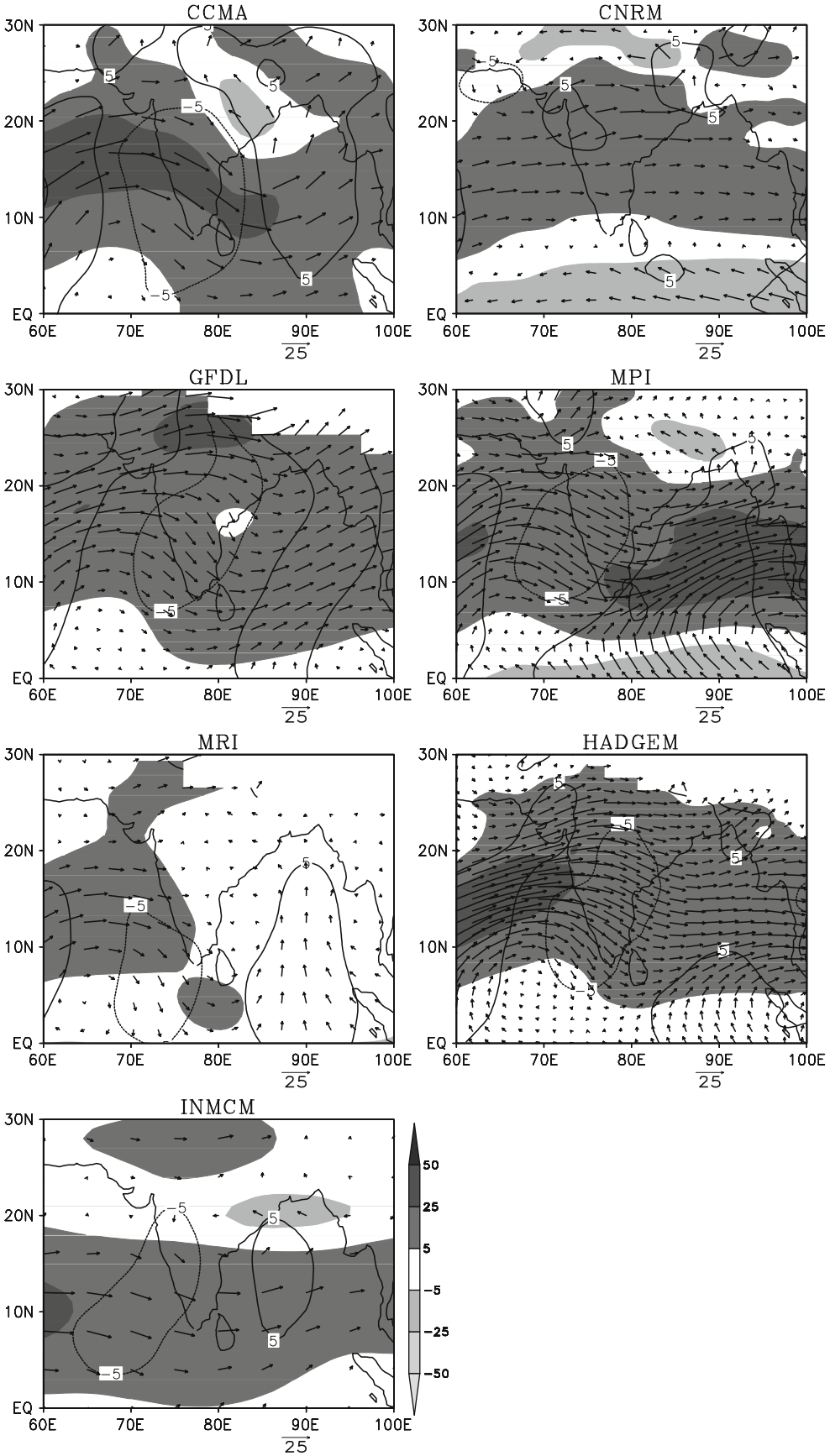

Fig. 15 Spatial patterns of projected 850 hPa moisture flux vector changes (A1B–20C3M) in ($kg^{-1}m^{-1}s^{-1}$). *Shaded* values are differences in zonal moisture flux and contour values are differences in meridional moisture flux

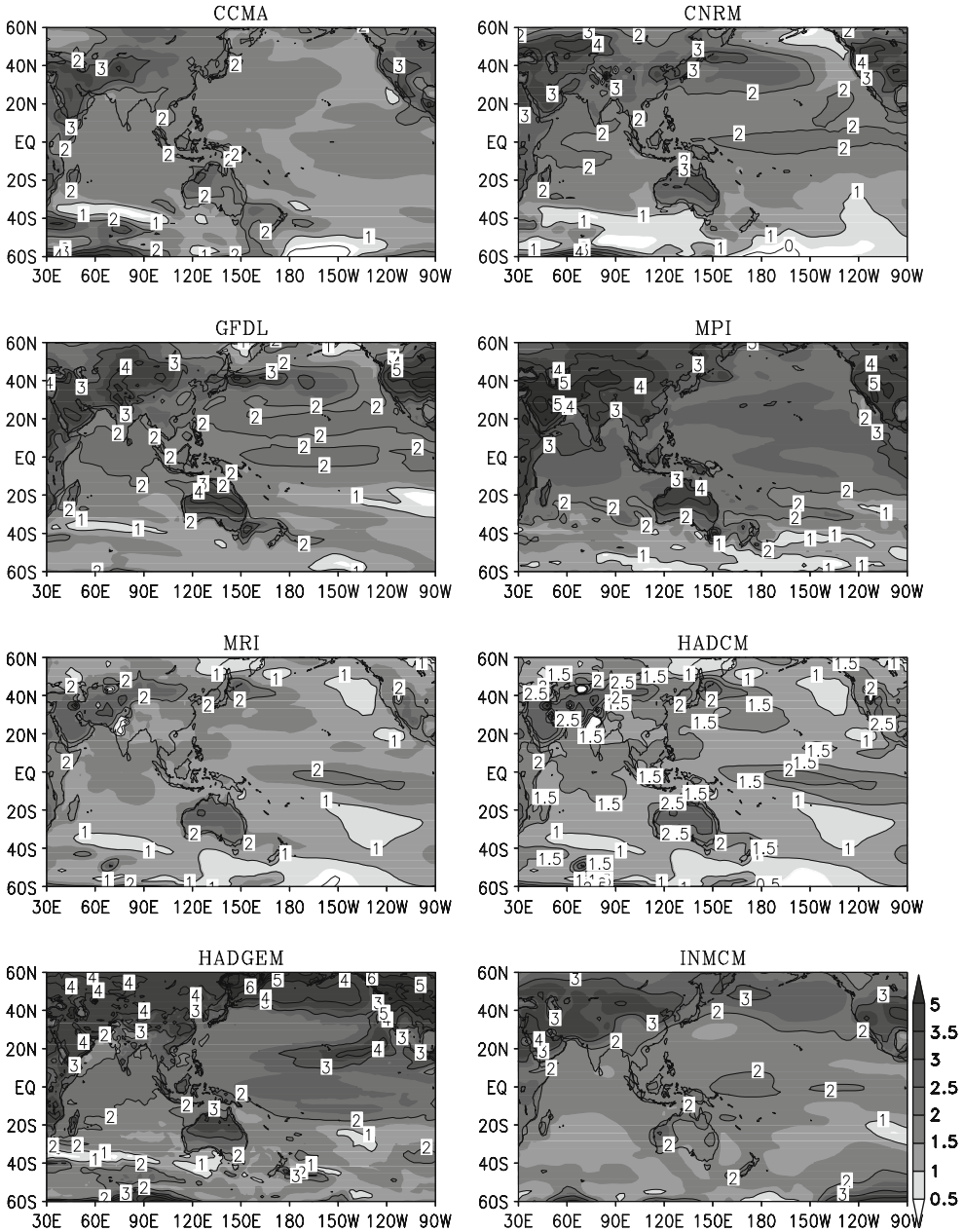

Fig. 16 Spatial patterns of projected surface skin temperature changes (A1B–20C3M) in °C

The projected surface temperature increase (Fig. 16) is large over the monsoon region, which increases the water holding capacity of the atmosphere to greater extent; whereby the hydrological cycle over the South Asian monsoon is enhanced in the A1B scenario in the model projections for the twenty-second century climate simulations. The homogeneous increase of surface temperature over the tropics in the models may have decreased the continental North South temperature gradient over the South Asian region, which could be a possible explanation for the decrease in the wind convergence in the A1B scenario.

We also investigated soil moisture fields (Fig. 17) available from five models (CCMA, MRI, HADCM, HADGEM and INMCM), which show a projected increase in soil moisture over the core Indian monsoon region, leading to increased precipitation recycling. The importance of the surface processes are also stressed in previous studies (Douville et al. 2002). We notice large increase in the projected soil moisture over western parts of India in MRI and HADGEM models (Fig. 17) compared with other three models. The soil moisture increase can be attributed to the increase in the precipitation due to increase in the lower tropospheric humidity increase and an enhanced precipitation recycling in these models.

We noticed that CCMA and MRI show a similar spatial feature in precipitation change while GFDL and MPI is another group in spatial similarity in precipitation in terms

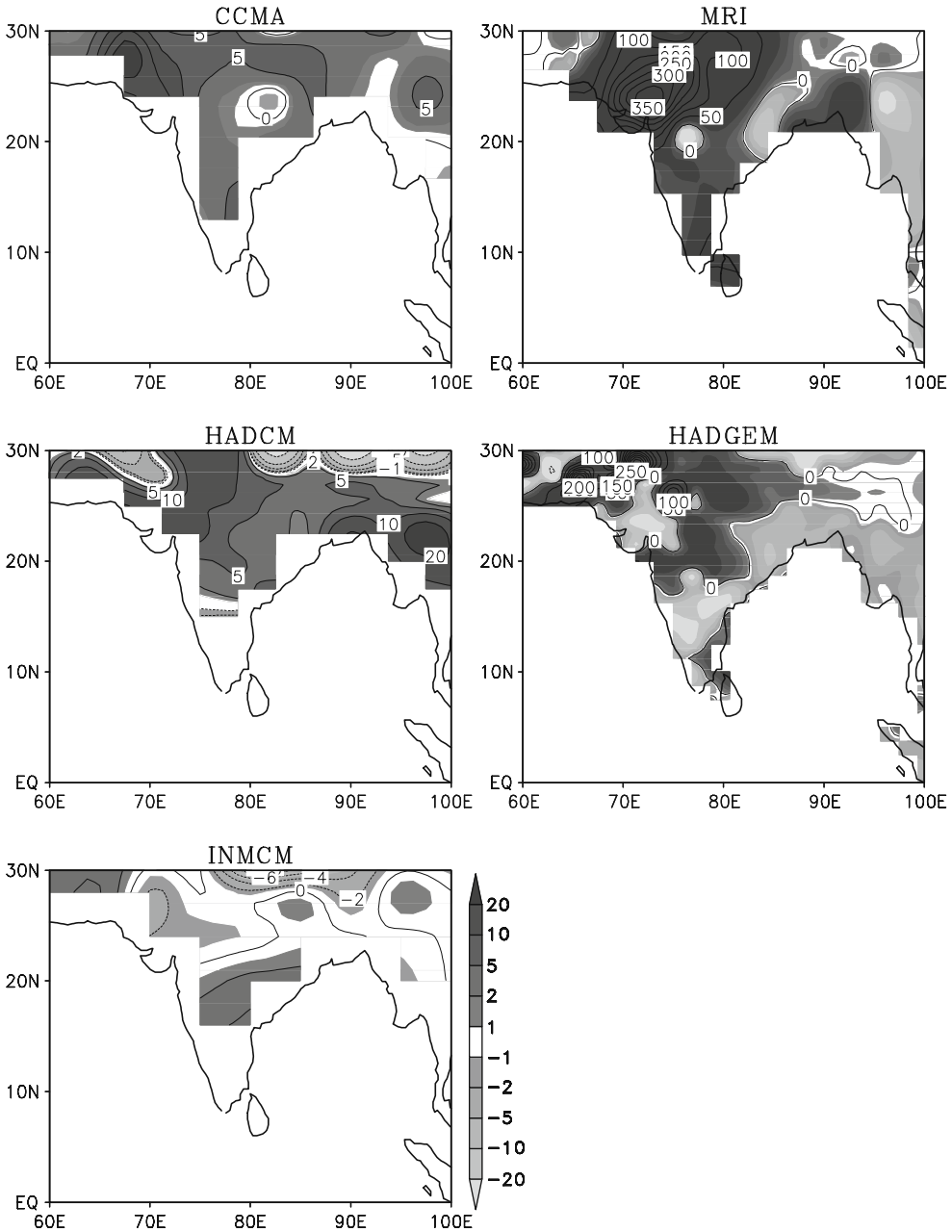

Fig. 17 Spatial patterns of projected surface soil moisture changes (A1B–20C3M) in percentage departure

of future projections in A1B scenario. These two major different patterns appear due to the circulation features in the models. The divergent circulation over the northwestern India in the models GFDL and MPI are strong compared with other models. The divergent circulation becomes even stronger in the A1B scenario leading to strong moisture divergence and reduction in precipitation.

5.2 Scenarios of variability of atmospheric water balance components

Apart from the changes in mean state, the likely changes in the variability of monsoon rainfall and water balance components in future will have profound impact on various facets of human activities as the year to year variability or otherwise known as the interannual variability of monsoon leads occasionally to large-scale drought and flood situations. Any increase in the variability will mean a more frequent occurrence of large-scale seasonal anomalies and associated drought and flood like situations. In view of this, we examined the likely changes in the variance of *P*, *C*, and *E* in the A1B scenarios from 2000 to 2200. The standard deviation is taken here to represent the variance of the P, C, and E and is computed on a 31-year sliding window during the entire period of simulations. The results are presented in

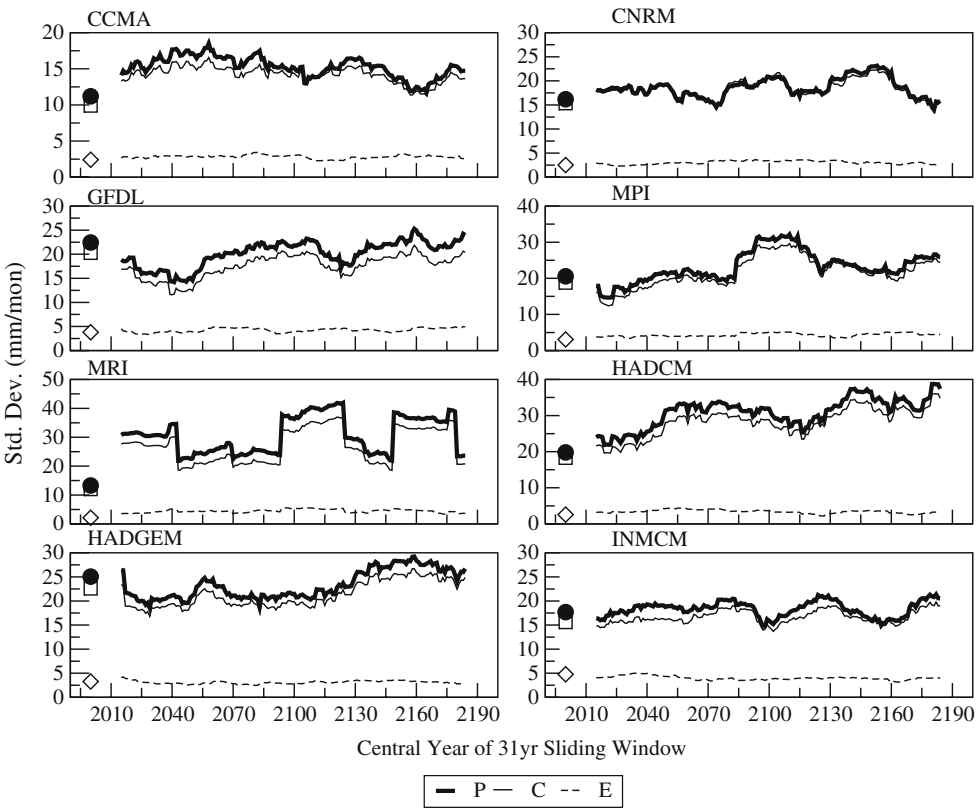

Fig. 18 Future changes in the variance (time series from 2000 to 2200) of AWB components (P, C and E) (mm/month) (standard deviation is taken as a measure of variability) of different models for A1B scenario run. The *dark-filled circles* denote 20-year (1980–1999) standard deviation of precipitation for respective models; similarly, *open squares* indicate standard deviation of convergence and *open diamond* indicate standard deviation of evaporation in 20C3M run

the form of time series of variance for the three components of water balance (*P*, *C* and *E*) for A1B simulation in Fig. 18. The standard deviation values for the 20C3M runs between 1980 and 2000 are also shown in Fig. 18 for comparison of changes in the variance of each water balance component (*P*, *C* and *E*). Most of the models show a general tendency of increased variance in the later part of twenty-first century. However, only a few models show such systematic increase in variance into the future. Therefore, it can be stated that there is as yet no conclusive evidence or a general consensus among models in the future changes of enhanced variability in monsoon rainfall.

6 Discussion and conclusions

This paper provides a brief description of the observed atmospheric water balance over the South Asian summer monsoon region and then proceeds to evaluate the performance of eight state-of-art coupled atmosphere-ocean general circulation models (AOGCMs) in their representation of regional characteristics of rainfall and atmospheric water balance over the South Asian summer monsoon region. Based on modelling experiments conducted for A1B scenario, regional climate change projections of rainfall and water balance components up to the end of the twenty-second century have been presented. The following are the major conclusions of this study:

1. The AOGCMs, despite their relatively coarse resolution, have shown a reasonable skill in depicting the observed hydrological cycle over the South Asian region. However, considerable biases do exist with reference to the observed hydrological cycle and also inter-model differences, which should be taken into account while interpreting the model projections.
2. Model simulations under scenarios of increased greenhouse gas concentrations indicate marked increase in both rainfall as well as atmospheric water balance components, particularly becoming obvious after the 2050s. There is considerable inter-model dispersion in the case of monsoon rainfall projections and atmospheric water balance.
3. Spatial patterns of rainfall change projections indicate maximum increase over northwest India, but changes in the atmospheric water balance components are generally widespread over the domain.
4. There is no clear evidence of substantial change in the variability of monsoon rainfall and atmospheric water balance over the next century.
5. While the scenarios presented in this study are indicative of the expected range of rainfall and atmospheric water balance changes, it must be noted

that the quantitative estimates still have large uncertainties associated with them.

6. Apart from the role of moisture convergence to the precipitation increase, evaporation too plays a role in the increase of precipitation through in situ surface hydrological processes.

The use of the 6-h interval instead of the model time step from the reanalyses raises questions on the quality of the moisture budget. The analysis is created at every 6 h in the reanalyses, the model used to create the first guess (6-h forecast) has a time step of 30 min, thus the fluxes accumulated during the 6-h intervals is best, but the whole calculations have much errors (analyses has errors, model has errors). However, the same calculations are done on a number of different reanalyses (NCEP/NACR, ERA-40, and JRA-25) to make sure that the best estimate is obtained. The data quality of the reanalyses, therefore, is guaranteed at this data-input time resolution, i.e. 6-hourly. The 6-hourly includes basically the diurnal cycle of circulation and convection, which guarantees fundamental quality of energy and water budget of the atmosphere.

Acknowledgment Authors would like to acknowledge many modelling centres for providing model simulation for about 200 years and also would like to acknowledge the PCMDI for archiving and providing the large datasets through their website (http://www-pcmdi.llnl.gov/). Authors would also like to acknowledge comments from anonymous reviewer for improving the paper. The diagrams used for this study have been prepared using the free software packages like GrADS, XMGRACE, Intel Fortran and computational work done on the Fedora Core operating system environment.

References

Adler RF, Huffman GJ, Chang A, Ferraro R, Xie P, Janowiak J, Rudolf B, Schneider U, Curtis S, Bolvin D, Gruber A, Susskind J, Arkin P, Nelkin E (2003) The version 2 global precipitation climatology project (GPCP), monthly precipitation analysis (1979–present). J Hydrometeor 4:1147–1167

Christensen JH, Hewitson B, Busuioc A, Chen A, Gao X, Held I, Jones R, Kolli RK, Kwon WT, Laprise R, Magaña Rueda V, Mearns L, Menendez CG, Raisanen J, Rinke A, Sarr A, Whetton P (2007) Regional climate projections climate change 2007: the physical science basis contribution of working group I to the fourth assessment report of the intergovernmental panel on climate change. In: S Solomon, Qin D, Manning M, Chen Z, Marquis M, Averyt KB, Tignor M, Miller HL (eds). Cambridge University Press, Cambridge. p. 996

Covey C, AchutaRao KM, Cubasch U, Jones P, Lambert SJ, Mann ME, Phillips TJ, Taylor KE (2003) An overview of results from the coupled model intercomparison project. Glob Planet Change 37:103–133

Delworth TL, Broccoli AJ, Rosati A, Stouffer RJ, Balaji V, Beesley JA, Cooke WF, Dixon KW, Dunne J, Dunne KA, Durachta JW, Findell KL, Ginoux P, Gnanadesikan A, Gordon CT, Griggies SM, Gudgil R, Harrison MJ, Held IM, Hemler RS, Horowitz LW, Klein SA, Knutson TR, Kushner PJ, Langenhorst AR, Lee HC, Lin SJ, Lu J, Malyshev SL, Milly PCD, Ramaswamy V, Russell J, Schwarzkopf MD, Shevliakova E, Sirutis JJ, Spelman MJ, Stern WF, Winton M, Wittenberg AT, Wyman B, Zeng F, Zhang R (2006) GFDL's CM2 global coupled climate models—Part 1: formulation and simulation characteristics. J Clim 19:643–674

Diansky NA, Volodin EM (2002) Simulation of present day-climate with a coupled atmosphere-ocean general circulation model. Izv Atmos Ocean Phys (Engl Transl) 38:732–747

Douville H, Chauvin F, Planton S, Royer JF, Salas-Melia D, Tyteca S (2002) Sensitivity of the hydrological cycle to increasing amounts of greenhouse gases and aerosols. Clim Dyn 20:45–68

Flato G, Boer GJ et al (2000) The Canadian center for climate modeling and analysis global coupled model and its climate. Clim Dyn 16:451–467

Hagemann S, Arpe K, Bengtsson L (2005) Validation of the hydrological cycle of ERA40. ERA-40 Project Report Series 24:42

Gadgil S, Sajani S (1998) Monsoon precipitation in the AMIP runs. Clim Dyn 14:659–689

Gates WL et al (1999) An overview of the results of the atmospheric model intercomparison project (AMIPI). Bull Am Met Soc 80:29–55

IPCC (1996) Climate change 1995: the science of climate change contribution of working group I to the second assessment report of the intergovernmental panel on climate change. In: Houghton JJ, MeiroFilho LG, Callander BA, Harris N, Kattenberg A, Maskell K (eds). Cambridge University Press, Cambridge. p. 572

IPCC (2001) Climate change 2001: the scientific basis contribution of working group I to the third assessment report of the intergovernmental panel on climate change. In: Houghton JT, Ding Y, Griggs DJ, Noguer M, VanderLinden PJ, Dai X, Maskell K, Jhonson CA (eds). Cambridge University Press, Cambridge. p. 881

IPCC (2007) Climate change 2007: the physical science basis contribution of working group I to the fourth assessment report of the intergovernmental panel on climate change. In: S Solomon, Qin D, Manning M, Chen Z, Marquis M, Averyt KB, Tignor M, Miller HL (eds). Cambridge University Press, Cambridge. p. 996

Johns TC, Durman CF, Banks HT, Roberts MJ, McLaren AJ, Ridley JK, Senior CA, Williams KD, Jones A, Rickard GJ, Cusack S, Ingram WJ, Crucifix M, Sexton DMH, Joshi MM, Dong BW, Spencer H, Hill RSR, Gregory JM, Keen AB, Pardaens AK, Lowe JA, Bodes-Salcedo A, Stark S, Searl Y (2006) The new Hadley centre climate model: evaluations of coupled simulations. J Clim 19:1327–1353

Jones C, Gregory J, Thorpe R, Cox P, Murphy J, Sexton D, Valdes H (2004) Systematic optimization and climate simulation of FAMOUS a fast version of HADCM3. Hadley Centre Technical Note 60. p. 33

Jungclaus JH, Keenlyside N, Botzet M, Haak H, Luo JJ, Latif M, Marotzke J, Mikolajewicz U, Roeckner E (2006) Ocean circulation and tropical variability in the coupled model ECHAM5/MPI-OM. J Clim 19:3952–3972

Kalnay E et al (1996) The NCEP/NCAR 40-year reanalysis project. Bull Amer Meteor Soc 77:437–471

Kang IS, Jin K, Wang B, Lau KM, Shukla J, Krishnamurthy V, Schubert SD, Waliser DE, Stern WF, Kitoh A, Meehl GA, Kanamitsu M, Galin VY, Satyan V, Park CK, Liu Y (2002) Intercomparison of the climatological variations of Asian summer monsoon precipitation simulated by 10 GCMs. Clim Dyn 19:383–395

Kripalani RH, Oh JH, Kulkarni A, Sabade SS, Chaudhari HS (2007) South Asian summer monsoon precipitation variability: Coupled climate model simulations and projections under IPCC AR4. Theor Appl Climatol 90:133–159

Lambert SJ, Boer GJ (2001) CMIP: evaluation and intercomparison of coupled climate models. Clim Dyn 17:83–106

Oki T, Musiake K, Matsuyama H, Masuda K (1995) Global atmospheric water balance and runoff from large river basins. Hydrol Processes 9:655–678

Onogi K, Koide H, Sakamoto M, Kobayashi S, Tsutsui J, Hatsushika H, Matsumoto T, Yamazaki N, Kamahori H, Takahashi K, Kato K, Ose T, Kadokura S, Wada K (2000) JRA-25; Japanese 25-year Reanalysis progress and status. Quart J R Meteorol Soc 131:3259–3268

Peixoto JP, Oort AH (1992) *Physics of climate*. Amer Inst Phys, New York, p 520

Prasanna V, Yasunari T (2008) Interannual variability of Atmospheric water balance over South peninsular India and Sri Lanka during North East Monsoon season. Intl J Climatol 28:1997–2009

Prasanna V, Yasunari T (2009) Time-space characteristics of seasonal and interannual variations of atmospheric water balance over South Asia. J Meteor Soc Jpn 87:263–287

Salas-Melia D, Chauvin F, Deque M, Douville H, Gueremy JF, Marquet P, Planton S, Royer JF, Tyteca S (2005) Description and validation of the CNRM-CM3 global coupled model. CNRM working note 103

Trenberth KE (1991) Climate diagnostics from global analyses: conservation of mass in ECMWF analyses. J Clim 4:707–722

Trenberth KE (1999) Atmospheric moisture recycling: role of advection and local evaporation. J Clim 12:1368–1381

Trenberth KE, Guillemot CJ (1998) Evaluation of the atmospheric moisture and hydrological cycle in the JRA-25 reanalyses. Clim Dyn 14:213–231

Trenberth KE, Fasullo J, Smith L (2005) Trends and variability in column integrated water vapor. Clim Dyn 24:741–758

Ueda H, Iwai A, Kuwako K, Hori ME (2006) Impact of anthropogenic forcing on the Asian summer monsoon as simulated by 8 GCMs. 698 Geophys Res Lett 33: L06703, doi:101029/2005GL025336

Uppala SM, Kallberg PW, Simmons AJ, Andrae U, da Costa Bechtold V, Fiorino M, Gibson JK, Haseler J, Hernandez A, Kelly GA, Li X, Onogi K, Saarinen S, Sokka N, Allan RP, Andersson E, Arpe K, Balmaseda MA, Beljaars ACM, van de Berg L, Bidlot J, Bormann N, Caires S, Chevallier F, Dethof A, Dragosavac M, Fisher M, Fuentes M, Hagemann S, Holm E, Hoskins BJ, Isaksen L, Janssen PAEM, Jenne R, McNally AP, Mahfouf JF, Morcrette JJ, Rayner NA, Saunders RW, Simon P, Sterl A, Trenberth KE, Untch A, vasiljevic D, Viterbo P, Woollen J (2005) The ERA-40 reanalysis. Quart J Roy Meteor Soc 131:2961–3012

Waliser DE, Jin K, Kang IS, Stern WF, Schubert SD, Wu MLC, Lau KM, Lee MI, Krishnamurthy V, Kitoh A, Meehl GA, Galin VY, Satyan V, Mandke SK, Wu G, Liu Y, Park CK (2003) AGCM simulations of intra-seasonal variability associated with the Asian summer monsoon. Clim Dyn 21:423–446

Wang B, Kang IS, Lee JY (2004) Ensemble simulation of Asian–Australian monsoon variability by 11 AGCMs. J Clim 17:699–710

Yukimoto S, Noda A, Kitoh A, Sugi M, Kitamura Y, Hosaka M, Shibata K, Maeda S, Uchiyama T (2001) The new meteorological research institute coupled GCM (MRI-CGCM2) model climate and variability. Papers Meteor Geophys 51:47–88